Explosive eruptions from the interaction of magmatic and hydrothermal systems during flank extension: the Bellecombe Tephra of Piton de La Fournaise (La Réunion Island)

Michael H Ort, Andrea Di Muro, Laurent Michon, Patrick Bachèlery

Explosive eruptions from the interaction of magmatic and hydrothermal systems during flank extension: the Bellecombe Tephra of Piton de La Fournaise (La Réunion Island)

Michael H. Ort[1] · **Andrea Di Muro**[2] · **Laurent Michon**[3] · **Patrick Bachèlery**[4]

Abstract Piton de la Fournaise (La Réunion Island) is a very active, primarily effusive ocean-island volcano. The Bellecombe Tephra represents at least three explosive eruptions that occurred between about 5465 and 2971 calendar years BP. Near the margin of the present-day Enclos Fouqué caldera margin, two Bellecombe eruptions produced a sequence of two tuff breccias interbedded with tuff. The tuff breccias only reach a few hundred meters outside the current caldera margin. At Petite Carrière, an old scoria cone ~1 km from the Enclos Fouqué margin, these two deposits (the "lower Bellecombe Tephra") are represented by two tuffs with incipient soil formation at the top of each. They are overlain by a third unit (the upper Bellecombe Tephra) made of bedded lapilli tuff and tuff, some reworked in small debris flows off the scoria cone. The lapilli increase in size and the beds in thickness southeastward, toward Chisny volcano and away from the Enclos Fouqué caldera. Deposits from the upper Bellecombe tephra are correlated to sites 5 km northwest of Petite Carrière and 6 km north of a postulated vent location on the north side of Chisny volcano. Distribution patterns of all Bellecombe tephra are consistent with eruption columns that did not rise above 8 km asl. The ash fraction of the Bellecombe Tephra contains three juvenile components: a dominant gray vitric basaltic ash, an oceanitic (olivine-rich basalt) ash, and pyroxene-bearing gabbro with a few percent glass. It also contains doubly terminated clear quartz grains, and olivine and rarer clinopyroxene crystals. The lower Bellecombe Tephra contains an altered brown ash, whereas a tan-yellow clay-rich ash is common in the upper unit. Lava flows of gray aphyric basalt and oceanite are exposed at the surface and preceded the Bellecombe eruptions, but the gabbro, quartz crystals, and hydrothermally altered grains indicate the involvement of the magma/hydrothermal system from 0.5- to 2-km depth. We propose that the three eruptions of the Bellecombe tephra were preceded by voluminous eruptions of lava flows that led to seaward-sliding mass movement of the volcano. This opened fractures that explosively depressurized the hydrothermal system and incorporated magma and gabbro, from the magma system and probably from rock along the fissure, in the ejecta. This model is consistent with the small erupted volume (150 Mm^3 for the lower two combined and about the same for the upper tephra) and presence of components from a variety of depths. If the eruption had excavated downward, more surficial components would be expected. Instead, the fissures allowed material from many depths to erupt simultaneously. Similar eruptions may occur after voluminous eruptions and/or when lateral seaward sliding of the volcano occurs.

Electronic supplementary material The online version of this article (doi:10.1007/s00445-015-0998-8) contains supplementary material, which is available to authorized users.

✉ Michael H. Ort
michael.ort@nau.edu

[1] SESES, Northern Arizona University, Box 4099, Flagstaff, AZ 86011, USA

[2] Observatoire Volcanologique du Piton de la Fournaise (OVPF), Institut de Physique du Globe de Paris (IPGP), Sorbonne Paris-Cité, CNRS, Université Paris Diderot, 97418 La Plaine des Cafres, France

[3] Laboratoire Géosciences Réunion, Université de La Réunion, Institut de Physique du Globe de Paris, Sorbonne Paris-Cité, UMR-7154 CNRS, 97744 Saint-Denis, France

[4] Laboratoire Magmas et Volcans, UMR CNRS-IRD 6524, Observatoire de Physique du Globe de Clermont-Ferrand, Université Blaise Pascal, 5, rue Kessler, 63038 Clermont-Ferrand, France

Keywords Piton de la Fournaise · Bellecombe Tephra · Hydrothermal eruption · Flank fracture

Introduction

The potential for explosive eruptions at dominantly basaltic effusive volcanoes on ocean islands has begun to attract attention recently, especially as the eruptive history of Kīlauea volcano (Hawaii, USA) over the past two millennia has been studied in greater detail (McPhie et al. 1990; Mastin 1997; Mastin et al. 2004; Swanson 2008; Fiske et al. 2009; Swanson et al. 2012a, b; 2015). Kīlauea is the most studied ocean-island volcano and has become, for many, the type example. At Kīlauea, most modern eruptions are effusive, producing lava flows and scoria and spatter cones, but Swanson et al. (2014) show that ~1500 out of the past 2200 years of activity at Kīlauea have been explosive, leaving only 700 years in which effusive edifice-building eruptions have been the norm. They argue that the Keanakāko'i (ca. 1500–1800 CE; Swanson et al. 2012a) and Uwēkahuna (ca. 200 BCE–1000 CE, including the Kulanaokuaiki Tephra Member, ca. 400–1000 CE; Fiske et al. 2009) formations were emplaced during periods of low magma supply rate and repeated phreatomagmatic explosive summit activity from deep calderas. During other periods, high magma supply rate filled the calderas and resulted in high volumes of lava effusion and edifice growth. Research at other ocean-island volcanoes has shown that types of activity not seen at Kīlauea are possible, such as the eruption of large volumes of silicic pyroclastic density currents (e.g., Martí et al. 1994). Piton de la Fournaise (La Réunion Island), one of the world's most active volcanoes, has many similarities to Kīlauea and has primarily produced effusive eruptions in historical time.

La Réunion Island, located on the Réunion hot spot about 800 km east of Madagascar (Fig. 1), consists of three volcanoes: (1) Piton des Neiges, the largest volcano on the island, active from at least 2.17 Ma to ca. 30 ka, which produced both basaltic lava flows and large-volume trachytic pyroclastic density currents; (2) Piton de la Fournaise, the currently active (~450 ka–present) volcano on the southeastern part of the island; and (3) Les Alizés volcano (>3.77 Ma to ~0.5 Ma), a large volcano that underlies Piton de La Fournaise (Merle et al. 2010; Lénat et al. 2012a). About 830,000 people live on the island and 450,000 tourists visit each year (Bachèlery et al. 2015).

Piton de la Fournaise (PdF) is a dominantly effusive volcano today, but evidence of past minor explosive episodes is abundant. Historic explosive events occurred, most notably in 1791, 1860, 1961, 1986, and 2007 CE, with concomitant crater collapse in the summit area. Modern (last 350 years) eruptive activity has typically involved magma ascending beneath the central cone and either erupting there or along the northeast or southeast rift zones. This results in effusive eruptions of hours to half a year in length, with small volumes (0.1–210 Mm^3) and rare weak ash plumes (Michon et al. 2013). A variant on this style is when flank eruptions lead to summit collapse and the formation of pit craters or summit calderas, in some cases accompanied by explosive activity. A third style of eruption is decades-long effusive eruptions associated with summit lava lakes. These long-term events were associated with explosive episodes in 1759, 1791, and 1860 CE. The deposits from modern explosive eruptions show possible evidence of the involvement of external fluids, such as lithic-rich ashes and breccias draping underlying lava flows and fountain deposits (scoria, Pele's hair, etc.). Notably, the modern deposits contain only sparse clasts from the geothermal system located ~500 m below the surface (Join et al. 2005; Lénat et al. 2012b). Michon et al. (2013) interpret that the explosions emanate from depths shallower than ~500 m. Evidence of explosive activity prior to 1759 CE includes breccia deposits along the Enclos Fouqué caldera rim and the more widely dispersed Bellecombe ash (Fig. 1; Bachèlery 1981; Mohamed-Abchir 1996; Mohamed-Abchir et al. 1998; Upton et al. 2000; Fontaine et al. 2002). We focus on this older activity because it may indicate what the volcano is capable of doing if the current effusive period transitions into a more explosive period. We show that PdF has experienced explosive eruptions in late Holocene time but with characteristics that are distinct from those at Kīlauea. We describe the deposits, interpret their origins, and use this to discuss potential future hazards.

Methods

Previous mapping identified most sections described in this work. Sections were either naturally occurring, in road cuts, or were exposed by digging pits. Sections were measured, described, and sampled in May and June of 2014. Carbon samples for dating were analyzed by CEA (Commissariat à l'énergie atomique) in Saclay, France, and data were calibrated to calendar years using the program Calib. The components of the ash fraction were identified with binocular microscope. Major element concentrations in the glassy tephra were analyzed using the WDS Cameca SX 100 electron microprobe at Laboratoire Magmas et Volcans, Clermont-Ferrand, France, with an accelerating voltage of 15 kV, a beam current of 8 nA, and a beam diameter of 20 μm to reduce Na loss. The beam current was reduced to 4 nA and the beam diameter to 10 μm when grains were too small for the 20-μm beam. The counting time was 10 s for Na, Ca, Ti, P, and Si; 20 s for Mg and Al; 30 s for Mn; and 40 s for Fe and K.

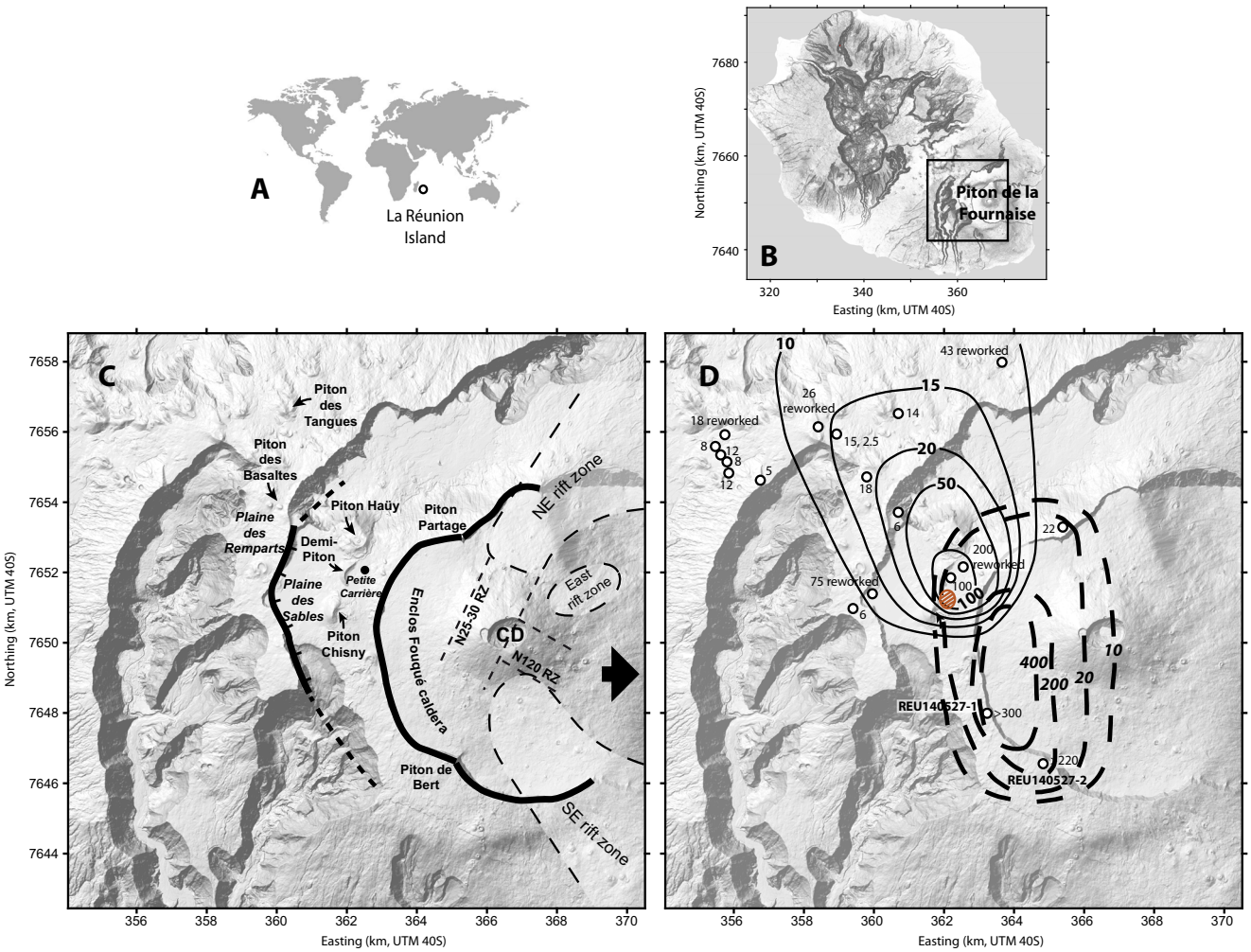

Fig. 1 **a** Location map of Réunion Island on world map; **b** digital elevation model (DEM) of Réunion Island showing the location of Piton de la Fournaise. **c** DEM showing the important geographic features of Piton de la Fournaise, including those referred to in the text. *Arrow* indicates direction of volcano extension. Rift zones contain many individual faults (see Michon et al. 2015, for details). *CD* Cratère Dolomieu. **d** DEM of same area as in **c**, with the site locations and isopachs (in cm) for the lower (*dashed*) and upper (*solid*) Bellecombe Tephra. Sites discussed in the text are marked. Hachured area south of Petite Carrière is possible vent area. Note that isopachs of the lower Bellecombe Tephra are very poorly constrained. Thickness at Piton des Basaltes site is likely an underestimate, as many layers or mixed reworked and primary deposits overlie the measured portion of the section

Results

Stratigraphic descriptions

Bachèlery (1981) and Mohamed-Abchir (1996) defined the Bellecombe Ash and showed that it has very different appearances at different localities. Medium to coarse tuff breccias and tuffs occur near the Enclos Fouqué (EF) caldera rim (Fig. 1), whereas ash and fine lapilli dominate within and to the west and north of the Plaine des Sables (west of EF caldera). Because the "Bellecombe Ash" includes tuff breccias but the word ash has size denotations, we propose to rename it the Bellecombe Tephra. This term includes all the different types of deposits within the unit and is thus more appropriate. Our work shows that these deposits record eruptions from two different vent localities that produced deposits with different physical characteristics and dispersal. Inside the Plaine des Sables caldera west of the EF rim, a complete section of the Bellecombe Tephra covers lavas around Demi-Piton cone and around a small scoria cone at Petite Carrière (Fig. 1). An oceanitic (melanocratic picritic magma with >20 % olivine and subordinate clinopyroxene crystals; Boivin and Bachèlery 2009) lava flow, dated at 3400 ± 1000 BP (He and Ne exposure dates; Staudacher and Allègre 1993; Supplementary Data Table 1) laps onto the weathered top of the scoria-cone deposit and underlies, with no evidence of weathering, the Bellecombe Tephra. This lava flow comes from a source now inside the Enclos Fouqué caldera, implying that the EF topographic depression did not exist at that time. The exposure age is stratigraphically consistent with a ^{14}C age

(5465 calendar years BP; Bachèlery 1981; Supplementary Data Table 1) for basal scoria below a lava flow underlying the Bellecombe Tephra in the uppermost part of the EF wall at the Pas de Bellecombe.

The deposit sequence is thickest and most complete in a small area between Petite Carrière and Demi-Piton cones. At Petite Carrière, the Bellecombe Tephra consists of a ~2.5-m-thick section of 18 cm of ash pellet and lapilli fallout overlain by 38 cm of massive and laminated fine ash beds with two one-clast-thick lapilli layers (together referred to hereafter as the lower Bellecombe Tephra), and an upper section consisting of a thick (1.5–2.5 m) indurated sequence of bedded lapilli and ash with abundant ash pellets, much of it reworked (hereafter referred to as the upper Bellecombe Tephra; Figs. 2 and 3). The basal 18 cm of the lower Bellecombe Tephra has abundant ash pellets and water escape structures (pipes and dish structures), implying it was very wet at the time of deposition. Channels within the primary beds in the overlying lower Bellecombe Tephra imply at least some available water at that time too. A ^{14}C age of 4696 ± 145 calendar years BP was obtained by Mohamed-Abchir et al. (1998) from uncharred twigs found near the base of the lower Bellecombe Tephra at Petite Carrière (Supplementary Data Table 1).

In the upper Bellecombe Tephra sequence of the Petite Carrière section, only the beds in the 155–196-cm interval appear to be entirely primary, with laterally continuous beds of moderately well sorted coarse ash and fine lapilli, interpreted as fallout (Figs. 2 and 3). Reworked beds (56–155- and 196–255-cm heights in Fig. 3), identified by erosive channels, rounded grains, and relatively few ash pellets, can be traced laterally to apparently primary deposits with

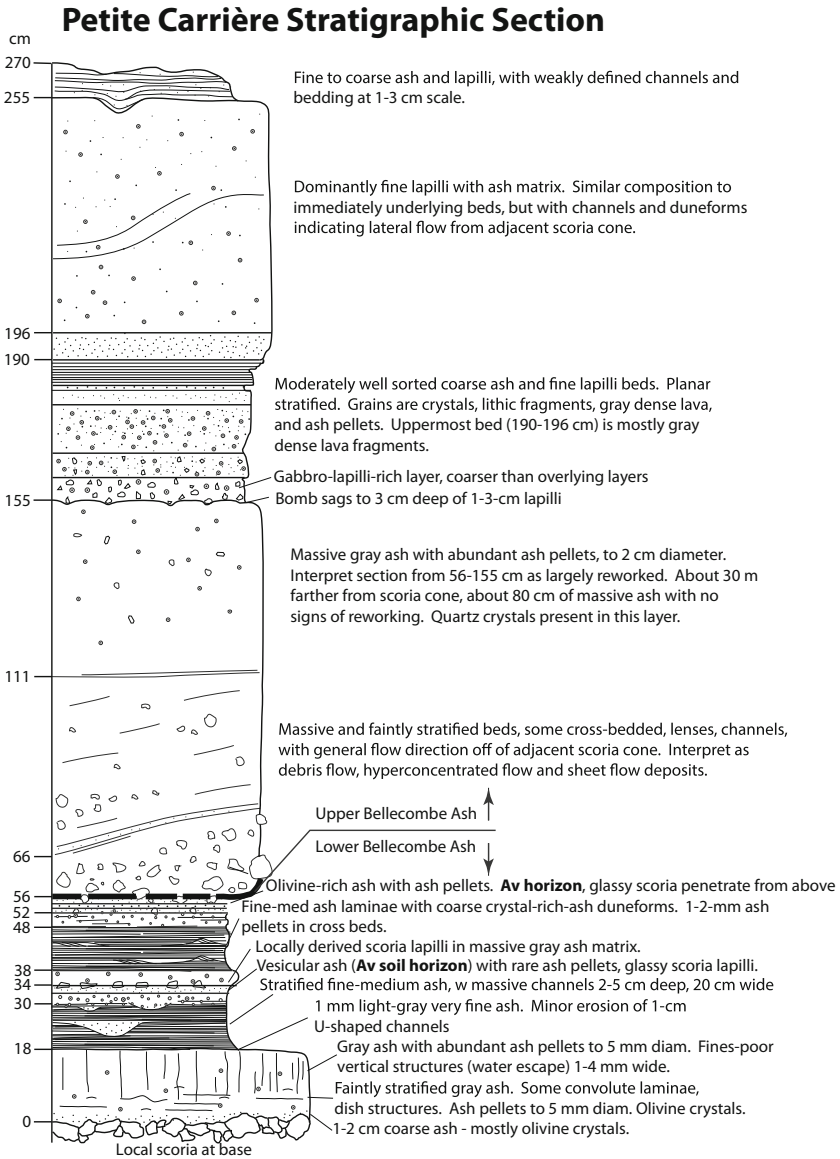

Fig. 2 Stratigraphic column of the Petite Carrière section. Location in Fig. 1

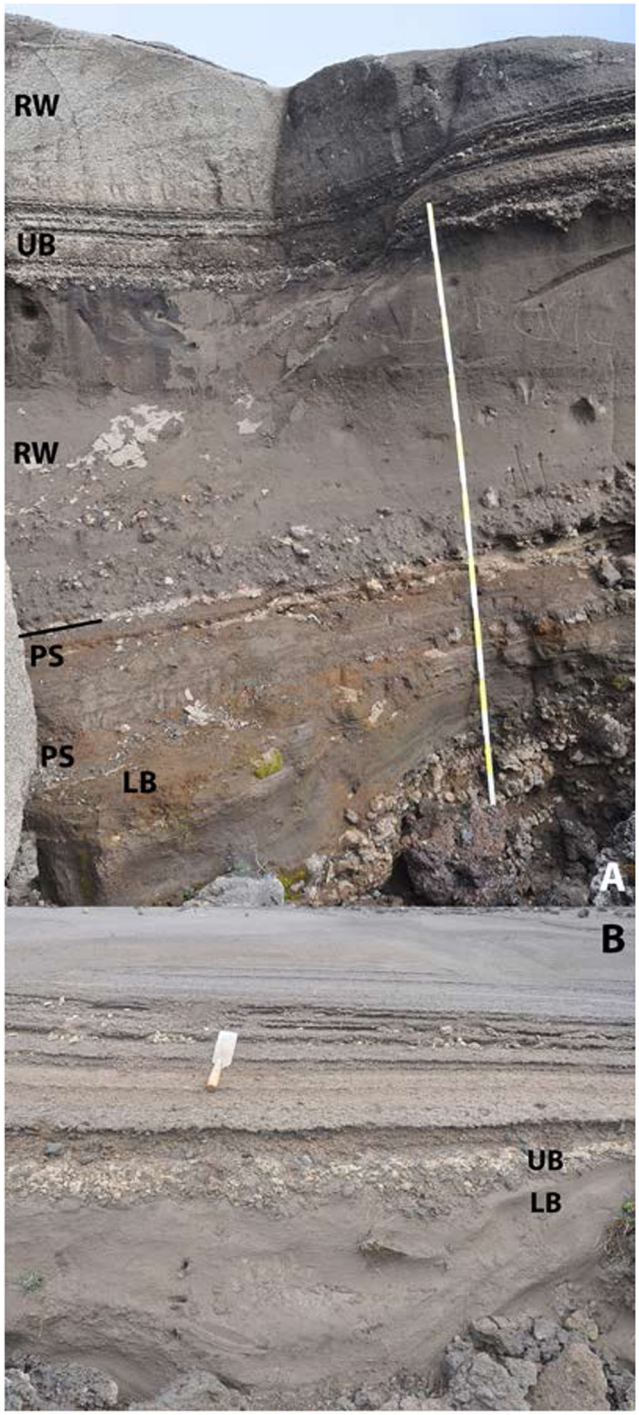

Fig. 3 Photos of **a** Petite Carrière and **b** Demi-Piton sections (locations in Fig. 1). *RW* reworked ash and lapilli, *PS* Av horizon paleosol, *LB* Lower Bellecombe Tephra, *UB* Upper Bellecombe Tephra. *Line* indicates contact between lower and upper Bellcombe Tephras. Scale is 2 m in **a**; trowel is 25 cm in **b**

horizontal laminae and beds and abundant ash pellets. Because the reworked beds lie within a sequence of primary deposits, the reworking appears to have occurred during the eruption itself. Most primary beds show signs of abundant water, including the presence of ash pellets and accretionary lapilli. Gabbro clasts and oceanite clasts, some with gabbro enclaves within them, occur sparsely in the upper Bellecombe Tephra above 155-cm height and free olivine and euhedral quartz crystals are abundant throughout the sequence.

Evidence for eruptive hiatuses and reworking of the deposits is present in both the lower and upper Bellecombe Tephra. The two one-clast-thick lapilli layers in the lower Bellecombe Tephra at Petite Carrière consist of scoria from the immediately adjacent small scoria cone and their undulatory contacts and stratigraphic position at the top of brown vesicular ash beds are interpreted to record significant hiatuses in tephra deposition (Fig. 3a). Two brown vesicular ashes within the lower massive and laminated fine ash beds are interpreted to be Av soil horizons from the incipient formation of a soil during significant depositional breaks (years to perhaps centuries), as their upper contacts are erosive and the lower contacts gradational. The vesicles are interpreted to result from surface sealing by water, after which a wetting front increases soil gas pressure as it propagates downward (Dietze et al. 2012). Fine to medium ash is an ideal grain size for forming vesicles when wetted thoroughly, as is often the case at PdF. Roots, which hinder gas pressure buildup and vesicle formation (Anderson et al. 2002), are absent in the ash. Lenses and channels within the upper Bellecombe Tephra reveal erosion and re-sedimentation off the adjacent scoria cone but do not require any significant hiatuses.

A similar stratigraphic section is continuously exposed over ~0.25 km^2 just west of Petite Carrière on a lava flow near the base of Demi-Piton (Fig. 3b). There, the lower Bellecombe Tephra is thinner (35–45 cm) than in the Petite Carrière section but present as several beds of massive gray ash with ash pellets. Above an undulatory contact, the upper Bellecombe Tephra is ~62 cm thick, with the lower 42 cm consisting of mostly clast-supported lapilli with a gray ash matrix, bedded at 1–6-cm intervals. Lapilli components include aphyric gray basalt, cored lapilli (palagonitic cores with gray ash covering them), red scoria, stained/altered basalt, gabbro, and oceanite (some of which enclose gabbro clasts). The beds are plane parallel and continuous, with moderate sorting and grain size varying between beds. These beds are overlain by about 20 cm of bedded matrix-supported lapilli tuff with dominantly gray basaltic and palagonitic clasts in a gray ash. The upper Bellecombe Tephra at Demi-Piton lacks the syn-eruptively reworked deposits present in the Petite Carrière section and therefore is thinner overall, but the lower 42 cm of the upper Bellecombe Tephra is considerably coarser at Demi-Piton, with clasts to 4 cm in diameter. Laminated reworked beds in braided channels, some with mud-crack structures, form the top of the sequence of Demi-Piton.

A distinctive coarse tuff breccia ("Bellecombe breccia" unit) occurs along the EF caldera rim of PdF, with ash beds above and below it (Figs. 1, 4, and 5a). The lapilli and blocks are a gray dense sparsely phyric basalt, many with partially

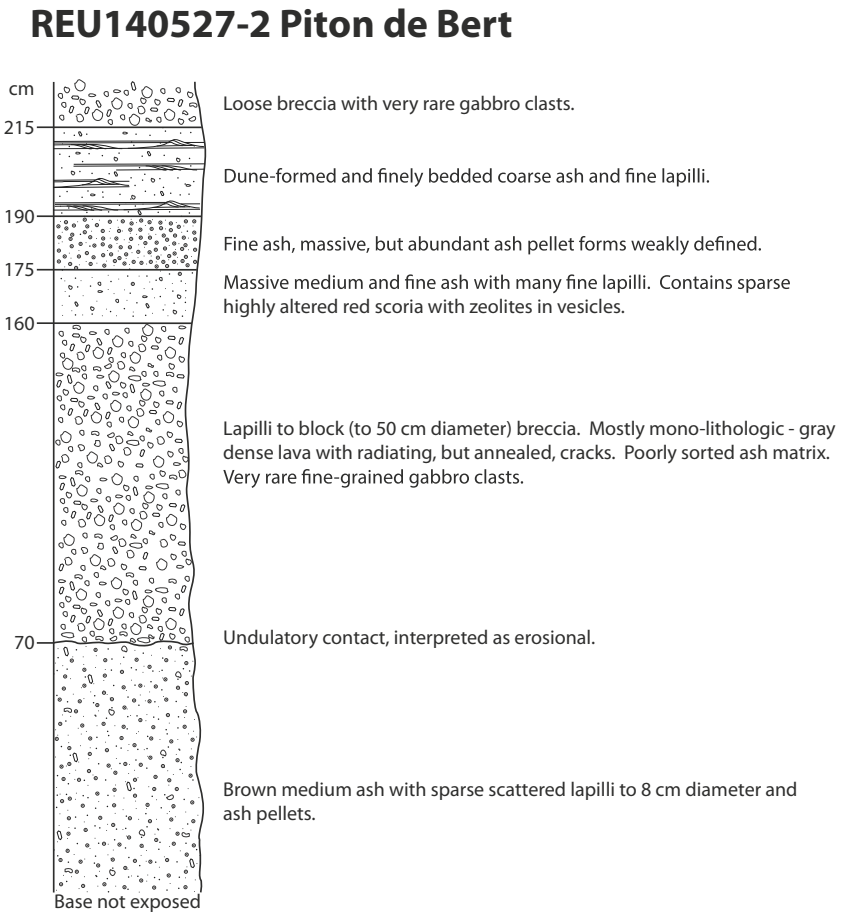

Fig. 4 Stratigraphic column of the Piton de Bert section (REU140527–2). Location shown in Fig. 1. At a nearby exposure, the brown ash overlies a lava flow

annealed cracks that penetrate into the clasts. Gabbro clasts occur throughout the tuff breccia, but range in abundance from common at site REU140527–1 to scarce at REU140527–2 (Fig. 1). It is not clear if these differences indicate they are deposits from two separate eruptions or simply record variable ejecta components erupted along a fissure vent. Beneath the tuff breccia is a massive, ash-pellet-rich gray fine to medium ash. Above the tuff breccia, the ash is bedded and variable in character. Some beds consist almost entirely of ash pellets, 0.2–1 cm in diameter, whereas other beds are massive ash with scattered fine lapilli, coarse ash with dune forms, and laminated fine ash. Euhedral, doubly terminated clear quartz crystals occur in all the ash. The cross-bedded coarse-ash deposits are interpreted as deposits of dilute pyroclastic density currents (PDC). The tuff breccia is found only within a few hundred meters of the caldera rim whereas the ash, 1–2 m thick in total, extends farther beyond the EF caldera in patchy outcrops. Based upon similarities in the ash components and stratigraphic position, we correlate the ash deposits of the EF caldera rim with the lower Bellecombe Tephra (lower 56 cm) at Petite Carrière.

On the northern rim of the EF caldera (Fig. 1), the Bellecombe breccia underlies a sequence of ash and lapilli beds named the "Partage sequence" by Morandi et al. (2016). This sequence groups the products of several eruptions, dated to the period 2971 ± 35 calendar years BP to 2129 ± 35 calendar years BP (Supplementary Data Table 1), that drape the inner part of the EF cliff (Morandi et al. 2016). Because there is a significant soil horizon between the Bellecombe and Partage sequences, they are considered separate units. The Partage dates provide a 2971 calendar years BP younger limit for the Bellecombe deposits described here.

Outside the Plaine des Sables caldera, on the Plaine des Remparts near Piton des Basaltes and Piton de Tangues, 2–4 km NW of Petite Carrière (Fig. 1), respectively, a single well indurated bed of ash and lithic lapilli, which we correlate with the upper Bellecombe Tephra of Petite Carrière, dominates or is the only primary bed in the Bellecombe sequence. Ash pellets to about 1 cm in diameter, many with irregular shapes, are abundant in the bed (Fig. 5b), as well as dense aphyric lava, gabbro, and altered lithic clasts to 1.5–2 cm in diameter. In the Piton des Tangues area (5 km northwest of Plaine des Sables), the upper part of the Bellecombe Tephra is weathered to form a black soil. Massive or laminated fine-grained ash layers occur above and below Bellecombe Tephra in many locations, some with locally derived red scoria lapilli that indicate reworking. Here, the Bellecombe Tephra is bracketed between pyroclastic deposits of two eruptions dated at 6356

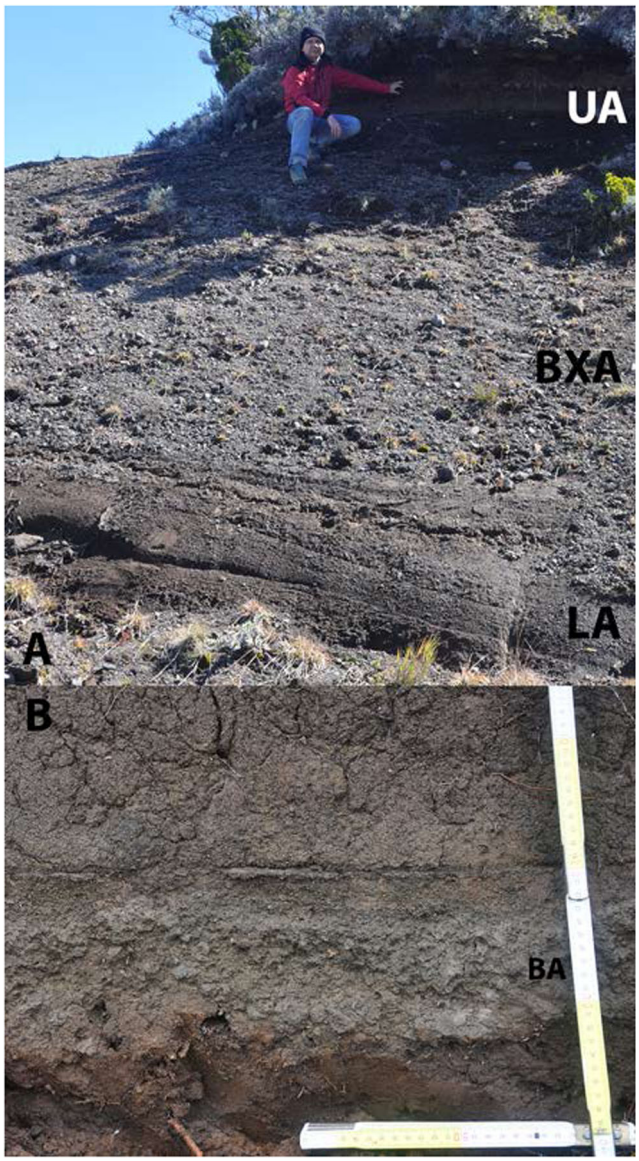

Fig. 5 Photos of **a** Enclos Fouqué rim (REU140527–1) and **b** Piton de Tangues sections (locations in Fig. 1). Note abundant ash pellets in ash. *LA* lower ash, *UA* upper ash, *BXA* breccia, *BA* Bellecombe Tephra (at Piton de Tangues, it is thought to be only the upper ash)

±35 (lower bed) and 3065±30 calendar years BP (upper bed; red lapilli fall) (Supplementary Data Table 1), consistent with the age range found in the proximal area.

Summary of Bellecombe Dates

The ^{14}C ages dates presented above suggest that the Bellecombe Tephra was emplaced in a time span between about 5465–2971 calendar years BP. The lower Bellecombe Tephra was emplaced soon after the eruption of a sequence of large oceanite flows, dated at 3400±1000 BP (He and Ne exposure dates; Staudacher and Allègre 1993; Supplementary Data Table 1) and the Pas de Bellecombe lava flow, dated at 5465±130 calendar years BP (Supplementary Data Table 1; Bachèlery 1981). These lava flows today form the uppermost western cliff of the EF caldera. The Partage Ash above the Upper Bellecombe Tephra dates to 2971 calendar years BP.

Components

The ash components of the two lower Bellecombe Tephra units are similar to one another but are distinct from components in the upper Bellecombe Tephra (Table 1). The lower Bellecombe Tephra at Petite Carrière and the matrix of the Bellecombe breccia at the sites by the Enclos Fouqué rim are marked by characteristic doubly terminated quartz grains, about 1 mm in size and <1 % of the total deposit. More than 85 % of the ash is a pale tan glass. White zeolite crystals are less than 1 % but stand out due to their color. Between 1 and 10 % of the grains are coarse ash to fine lapilli of fresh medium-gray basalt. These are typically dense and angular and appear to be the same material as the clasts in the tuff breccia ("Bellecombe breccia") that is associated with the ash deposits. Uncommon oceanite and brown-stained gabbro grains occur throughout the ashes. In the upper ash deposit of the Bellecombe breccia at Piton de Bert (along the southern cliff of the EF caldera), a brown ash similar in color to the gabbro grains makes up about 5 % of the total.

The glass has a chemical composition similar to that of the most recent aphyric basalts of Piton de la Fournaise (Fig. 6, Table 2), with the exception of the glass sampled between 48 and 52 cm above the base, which spans a broad range of low Ca/Al_2O_3 at almost constant MgO contents. All glass compositions are evolved (MgO 6.8–4.2 wt %). The glass composition in the upper Bellecombe Tephra plots at the upper end of the trend documented by Upton et al. (2000) for glass in gabbro clasts in the Bellecombe Tephra. Glass in the lower Bellecombe Tephra is more chemically heterogeneous, possibly because of the occurrence of fragments reworked by the underlying scoria cone (basal unit) and ash coming from other vents (incorporated into the Av layer).

The upper Bellecombe Tephra is marked by two types of ash grains (Table 1)—a light to medium gray one and a tan-yellow one—that form the matrix of the deposit in the coarse proximal sites and the entire deposit at distal sites. The yellow ash is pervasively altered—not just a stain on the outside—and has abundant clay minerals. The gray ash is finely vesicular, angular, and fresh and is interpreted as the magmatic component of the upper Bellecombe eruption. Crystals are abundant olivine (in coarser deposits it forms glomerocrysts, in some cases with clinopyroxene), quartz (clear, doubly terminated), and rare clinopyroxene. Gabbro grains, fine lapilli to coarse ash in size, occur in the Petite Carrière area but are less abundant at Piton de Tangues and do not occur at Piton Sec (at 5 km northwest and 6 km west of the Plaine des Sables,

Table 1 Grain components in the Bellecombe Tephra

	Gray Vitric	Gabbro	Olivine	Quartz	Zeolite	Comments
Lower Bellecombe near Enclos Fouqué and Petite Carrière	~1–10 %, blocky angular, fresh	1–2 %, brown staining	1–2 % (+ lesser clinopyroxene, Fe-Ti oxide)	1 %, doubly terminated, 1 mm	<1 %, but bright white so obvious	85 % pale tan ash, same composition as recent aphyric basalts
Upper Bellecombe Petite Carrière	Two ash types: 5–70 % dark gray, finely vesicular. 15–90 % yellow fine ash coats all grains, 1–2 % coarse yellow ash	1–5 % at Petite Carrière, decrease in abundance with distance	1–5 % typical, 10–15 % in some beds. Clinopyroxene <<1 % but ubiquitous	<1 % typical, 15–20 % in some beds, to 1 mm.	None	Many variations in components because many individual beds. Yellow ash is clay rich

respectively), perhaps due to fining of the deposit. Single crystals from the gabbro are medium ash in size, so sorting may have removed multicrystal aggregates.

Discussion

Deposit correlation and vent locations

At least three explosive periods are represented by the Bellecombe Tephra, with a significant hiatus between each. The lower Bellecombe Tephra at the Petite Carrière site contains two incipient soils, one in the middle and one at the top, that indicate depositional breaks (Figs. 2 and 3). No evidence of an eruptive hiatus is apparent in the upper Bellecombe Tephra, although syn-eruptive reworking is evident near the scoria cone. The ash components can be used for correlation. The lower Bellecombe Tephra at Petite Carrière correlates with ash in the tuff breccia and tuff beds in the Bellecombe breccia along the EF border (sites REU140527–1 and REU140527−2). The depositional hiatus within the lower Bellecombe Tephra at Petite Carrière may correspond with the erosional contact in the REU140527–2 Piton de Bert section. The lower Bellecombe Tephra appears to record at least two explosive eruptions from near the western wall of the EF caldera, as the deposits thin and fine abruptly away from there. The source of the oceanite lava flows that underlie the lower Bellecombe Tephra is within the current EF depression, suggesting that the caldera was not yet formed at that time.

Medium-grained lapilli tuffs within the upper Bellecombe Tephra only occur near Demi-Piton (Fig. 2), suggesting that these are the most proximal outcrops of that unit. The northern flank of Chisny is the best vent possibility, as the lava flows there are younger than the Bellecombe Tephra (Morandi et al. 2016) and would cover any evidence of the vent, whereas Demi-Piton lava flows underlie the Bellecombe Tephra near Petite Carrière but no evidence of a vent is seen.

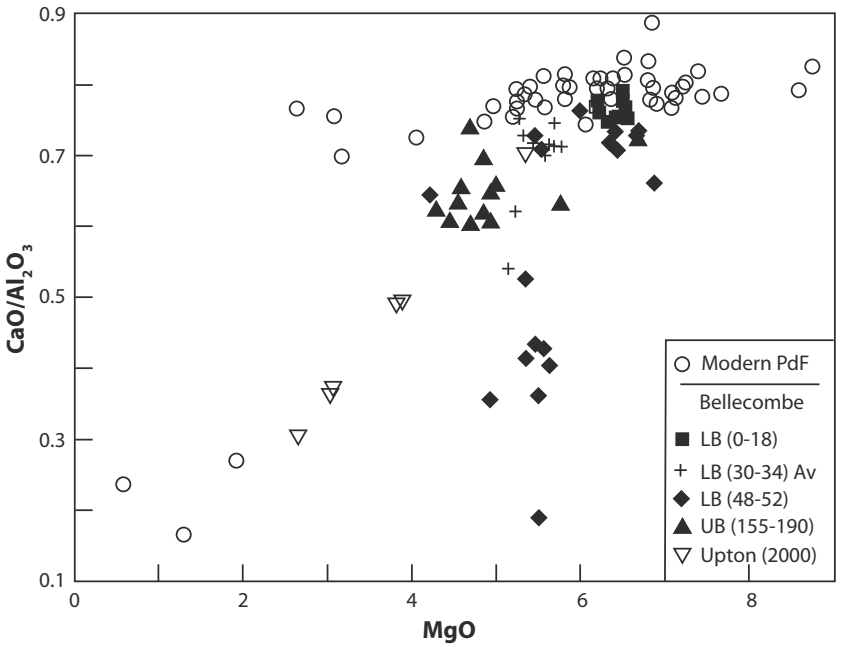

Fig. 6 CaO/Al_2O_3 vs. MgO data for ash grains from the Bellecombe Tephra at Petite Carriere, with sampling heights shown for each symbol. The 30–34-cm sampling height is of the Av soil horizon. Data are from this study and from Upton et al. (2000). The modern PdF data are from the Observatoire Volcanologique du Piton de la Fournaise unpublished data base

Table 2 Average chemical compositions of Bellecombe Tephra glass from microprobe analysis of samples from the Petite Carrière section

Bellecombe	LB-Base	LB-Av	LB	UB
Layer	BAM1	BAM3	BAM6	BAM9
Depth range	0–18	30–34	48–52	155–190
n	34	14	15	13
SiO_2	48.68	48.58	49.05	49.59
TiO_2	2.81	3.24	3.38	3.31
Al_2O_3	14.49	14.55	14.59	14.76
FeO*	10.79	11.33	11.96	11.12
MnO	0.17	0.19	0.18	0.20
MgO	6.38	5.72	5.66	4.94
CaO	11.20	10.38	8.05	9.60
Na2O	2.69	3.13	3.96	3.27
P2O5	0.34	0.45	0.47	0.54
K2O	0.77	1.07	1.50	1.30
Total	98.34	98.65	98.78	98.62

Depth range is sampling horizon, in centimeters above the base; n = number of averaged analyses; FeO* is total Fe as FeO

Clast types and sources in the volcanic system

The lower and upper Bellecombe Tephras have distinctly different ash types and vent areas and are separated in time, so we consider their origins separately, starting with their components.

The abundant gray ash in all deposits is interpreted to represent a magmatic component. In the tuff breccias, the gray lava lapilli and bombs commonly have breadcrust textures, implying that they were hot and vesiculating at the time of the eruption, consistent with a juvenile origin. The oceanite lava flows, clasts of which are common in the Bellecombe Tephra, may have been incorporated from the pre-Bellecombe lava flows. The very high abundance of free olivine crystals in the Bellecombe Tephra probably reflects the high olivine content of typical oceanites. Therefore, olivine-rich oceanite magma might represent a second "juvenile" component. Closely spaced (in time and location) eruption of aphyric and crystal-rich magma was documented during the major 2007 caldera-forming eruption (Di Muro et al. 2014). Upton et al. (2000) interpreted the gabbro xenoliths as evidence of a nearly crystalized magma body ≥2000 m below the surface. They describe a few percent glass in the xenoliths, which they interpret as residual melt. Thus, these gabbro xenoliths were comagmatic and still hot and could be considered a third "juvenile" component. Famin et al. (2009) and Di Muro et al. (2014) use melt inclusion compositions in olivine crystals from eruptions in 2005 and 2007, respectively, to show a shallow (<1.8 km) depth of origin for the olivine crystals in the oceanites and argue that less phyric basalts come either from the upper portion of the plumbing system (above 1.8-km depth) or record new deep recharge events. The evolved (for PdF) glass compositions of ash in both the lower and upper Bellecombe Tephra (Fig. 6, Table 2) are in agreement with a shallow origin for the magma that triggered the eruptions. Both crystal-rich and crystal-poor magma types can come from the same shallow magma body ($P < 200$ MPa) and the olivine-rich gabbro clasts may represent more crystallized portions of this same magma differentiation zone. Thus, the three inferred juvenile components could have come from the same magma body, physically mixing during eruption.

Several lines of evidence suggest that the altered grains come from a hydrothermal system above the magma storage zone. The doubly terminated quartz grains do not occur in basaltic lava of PdF but, based on fluid inclusion data, form in the hydrothermal system a few hundred meters below the PdF summit area (Mohamed-Abchir et al. 1998; Lénat et al. 2000; Fontaine et al. 2002). Bret et al. (2003) studied the hydrothermal alteration minerals exposed along a tunnel through Piton des Neiges, finding that crystallization of zeolite and clay is strongly controlled by hydrothermal fluids. Zeolite predominates over clays in the unsaturated zone above the water table, but clay is the only alteration mineral, and very abundant, within the saturated zone. These alteration-mineral facies develop because of outgassing and pH changes and should be applicable to other volcanoes, especially one as similar as PdF, a few kilometers away. Lénat et al. (2000) and Join et al. (2005) show this system at PdF is currently shallowest beneath Cratère Dolomieu, the active central cone in the middle of the Enclos Fouqué, where most summit eruptive activity is now located. Join et al. (2005) show that the water table is at 1500 m asl beneath the Plaine des Sables, about 600 m below the surface, consistent with outcrops in the deep valley near Grand Pays (Fontaine et al. 2002). Based on the geoelectrical signal (Lénat et al. 2000), the hydrothermal system beneath Plaine des Sables is marked by abundant clays and alteration products, consistent with the findings of Bret et al. (2003). Bachèlery and Mairine (1990) and Lénat et al. (2012a) assert that the Piton de la Fournaise edifice was first built with a focus in the Plaine des Sables area and later moved to its current location 5–6 km farther east. Their model implies a large, perhaps now partially fossilized, hydrothermal system under Plaine des Sables similar to that currently under Enclos Fouqué. The hydrothermally altered grains in the Bellecombe Tephra likely come from this system. The precise depths of the magma and hydrothermal systems likely vary spatially and temporally, but the similarity of magma types over time suggests that the systems themselves persist.

The lower Bellecombe Tephra includes grains from at least three parts of the postulated magma complex and the nonsaturated zone of the hydrothermal system beneath PdF, whereas the upper Bellecombe Tephra also includes hydrothermally altered, clay-rich wall rock material from the saturated part of this system. The lower Bellecombe Tephra contains abundant dense juvenile lava clasts with jigsaw cracks,

many partially annealed by the heat of the clast. The lava had outgassed significantly and these clasts may represent part of a feeder dike network that was ejected during the explosions. The deeply altered clay-rich grains of the upper Bellecombe Tephra are notably absent from the lower Bellecombe Tephra, but the quartz and zeolite crystals in the lower Bellecombe Tephra imply the involvement of the nonsaturated zone of a hydrothermal system.

During the Bellecombe eruptions, phreatomagmatic explosions produced tuff breccias, wet pyroclastic density currents, and ash fall. The tuff breccias are only exposed along the EF rim and fine rapidly away from there, implying both limited mobility and a source within the Enclos Fouqué. The upper Bellecombe Tephra contains abundant hydrothermally altered clay grains, indicating involvement of a more mature hydrothermal system and a greater depth (below the water table) in that system than during the eruption of the lower Bellecombe Tephra.

The fine-grained and laminated nature of many beds in the upper Bellecombe Tephra is consistent with deposition from an ash-rich misty cloud or ash rain, while ash pellets may reflect somewhat less wet conditions (Schumacher and Schmincke 1995; Rose and Durant 2011). Clouds and mist are daily occurrences in the summit area for much of the year, so external water for these features could come from phreatic water involved in the eruption or from low clouds above the vent area.

The inferred vent area for the upper Bellecombe Tephra, on the northern flank of Piton Chisny, is along an alignment of vents (Fig. 1). Demi-Piton, Piton Chisny, and Piton Haüy may lie atop a roughly N-S fracture system (Lénat el al. 2000) that could provide a preferred pathway for magma and for hydrothermal fluids. We speculate that this fracture system represents the pathway of magma ascent feeding these three large cones as well as the vent for the upper Bellecombe Tephra.

The abundant hydrothermal clay grains in the upper units are indicative of involvement of country rock from a few hundred meters depth in the water-saturated core of the hydrothermal system under Plaine des Sables (Lénat et al. 2000, 2012a; Join et al. 2005). It is worth noting that, below the saturation level, water pressure increases in low permeability terrains and may significantly contribute to physical conditions that are favorable for triggering landslides (Iverson 1995). Thus, the saturation level is critical in determining the mechanical state of the interior of volcanoes. The involvement of saturated rocks in the Bellecombe Tephra may be related to lateral sliding at the time of the eruption.

Volumes and column height

Volumes for the two Bellecombe units were estimated using isopachs based upon the limited number of sections that exist and the methods of Bonadonna and Costa (2012, 2013) (Supplementary Data Fig. 1). The lower Bellecombe Tephra, which includes two or more breccia units separated by an incipient soil, has a maximum total volume of about 1.5×10^8 m^3 (not DRE, a calculation complicated by the presence of at least three different "juvenile" types and abundant lithic fragments). We interpret that much of the lower Bellecombe Tephra was ballistically emplaced, as it contains many dense clasts of coarse lapilli size that are much larger than the rest of the deposit. In such a case, the Bonadonna and Costa (2012, 2013) method may not be reliable. A simple calculation of the amount of material within each isopach, ignoring the outermost extrapolated isopach (assuming that the deposit thins rapidly), yields 5.9×10^7 m^3 (not DRE). The upper Bellecombe Tephra has a volume of about 1.4×10^8 m^3, but this assumes a "normal" decrease in deposit thickness. The abundance of ash aggregation features (ash pellets, ash laminae interpreted from wind-blown mist) implies that the ash may have been scrubbed from the plume quickly. If so, the modeled thinner isopachs may be less extensive than typical in a dry eruption. The uncertainty of both volume estimates is large, given the paucity of sites and uncertainty about aerial extent of the deposits. Because of the abundance of lithic grains in the deposits and the low density, the dense rock equivalent values are probably about a third of the volumes given above, or around 5×10^7 m^3 for both deposits. This volume is typical of some of the largest recent effusive eruptions of Piton de la Fournaise (Roult et al. 2012).

The eruption columns that produced the Bellecombe Tephra were of limited height. Estimation of column height using isopleths is unreliable for the Bellecombe Tephra because of limited outcrop distribution. The very limited dispersal of the lower Bellecombe Tephra, with no deposits recorded farther than ~1 km from the Enclos Fouqué margin, is consistent with a very low column and ballistic emplacement of much of the coarse material. The ash eruptions of the upper Bellecombe Tephra were small in volume but had a convecting column in order to deposit fine ash >5 km from the vent area. Counterclockwise rotation of wind direction is well known on La Réunion Island, and its effect has been recently documented during the large 2007 eruption (Tulet and Villeneuve, 2011). Modeling of ash plumes from PdF (by Barsotti and de Michieli Vitturi, reported in Di Muro et al. 2015) confirms 2007 observations that trade winds carry ash to the west and northwest at lower altitudes but winds from the west dominate in higher columns. No Bellecombe Tephra has been found to the east of the summit area. The preserved distribution of the upper Bellecombe Tephra is consistent with observations and modeling, which suggest plume height above 7–8 km asl (5–6 km above the vent area) is unlikely. Columns higher than that would deposit far more tephra to the east. Using the eruptive volume, a 6-km plume height and the plume models of Mastin et al. (2009) and Sparks et al. (1997) yields fluxes of 95 and 139 m^3/s and eruption lengths of 2.0 and 1.4 months, respectively. With

eruptive breaks to produce the bedded deposits, this may be an underestimate of the eruption length.

Conduit system and related volcanic structure

The eruptions of the lower Bellecombe Tephra were largely punctuated explosions ejecting ballistic blocks and lapilli, interspersed with low columns that deposited wet ash via fallout and weak pyroclastic density currents. Most of the components in these deposits come from shallow levels (upper 500 m) in the volcanic edifice—hot gray lava blocks and ash and quartz crystals from the upper hydrothermal system. The rare gabbro ash and lapilli come from deeper in the edifice, probably >1 km. The eruption that produced the upper Bellecombe Tephra dominantly ejected ash from the subvolcanic pluton and magma body and the surrounding hydrothermal system, indicating source depths from 2.5- to 0.5-km depth. In both the lower and upper Bellecombe Tephra, the grains come from all sources from the start of eruption and were supplied throughout eruption, indicating that the eruption started at those depths. A simple crater modeled as an inverted cone with 45° sides to a depth of 500 m would be 1 km in diameter and have a volume of 0.13 km^3, about three times larger than the total erupted volume for the both units of the lower Bellecombe Tephra and not deep enough for the upper Bellecombe Tephra. In addition, it would take an enormous explosive force to excavate such a crater in one explosion, and the deposits would be dominated by the rock types nearest the surface rather than those at depth.

A fracture or fault that opened by seaward movement of the volcanic edifice is a much simpler explanation. The eastern flank of Piton de la Fournaise has a sliding rate of 1–3 cm/year and accelerates during major distal eruptive events (Brenguier et al. 2012). In the case of the Bellecombe eruptions, we speculate that sliding of the edifice allowed depressurization of the hydrothermal system, which gave the explosive impetus for the eruptions and likely also contributed to the high water contents in the eruptive plume. This is consistent with the N-S clast dispersion of the lower Bellecombe Tephra, which roughly corresponds to the orientation of the NE-SW rift zones crossing the Enclos Fouqué and bounding the eastern mobile flank. Because the conduit was opened by tectonic processes, the overburden was not an obstacle and the ejecta came from depths of 2.5 to 0.5 km due to sudden depressurization of the magma and hydrothermal systems. Based upon the abundance of oceanite clasts and olivine crystals, one or more large oceanite lava eruption(s) may have preceded the emplacement of both the lower and upper Bellecombe Tephra. Recent minor caldera-collapse events, such as in 2007 (Michon et al. 2007; Fontaine et al. 2014; Di Muro et al. 2014), have been associated with eruptions on the lateral flank of PdF, and Michon et al. (2013) show that lateral magma drainage is associated with summit phreatomagmatic activity. The larger Bellecombe eruptions may have had correspondingly large lateral drainage and collapse or slides, creating a fissure for the eruption. Lénat et al. (2000, 2012a) and Fontaine et al. (2002) have postulated significant normal faults under both the western Enclos Fouqué (either at the caldera margin or a kilometer inside of it) and the Plaine des Sables, about where we place the two vents for the Bellecombe Tephra. Piton Chisny, Demi-Piton, and Piton Haüy may align along the fault in Plaine des Sables, or the explosive eruptions could have occurred along a fault related to the caldera margin at the edge of Plaine des Sables. The low column heights of the Bellecombe eruptions are consistent with a deep eruption locus and low temperature of the eruptive mixture.

Bellecombe eruption model

The lower Bellecombe Tephra eruptions occurred after eruptions that produced oceanite lava flows. The outpouring of lava, whether in the summit area or on the flanks, led to caldera collapse and possibly lateral movement along faults identified in the Enclos Fouqué caldera (Michon and Saint-Ange 2008) (Fig. 7). Sudden release of pressure from the shallow portion of the then-young hydrothermal system, centered around what is now Cratère Dolomieu, caused explosions that ripped up portions of the lava section, quartz from the

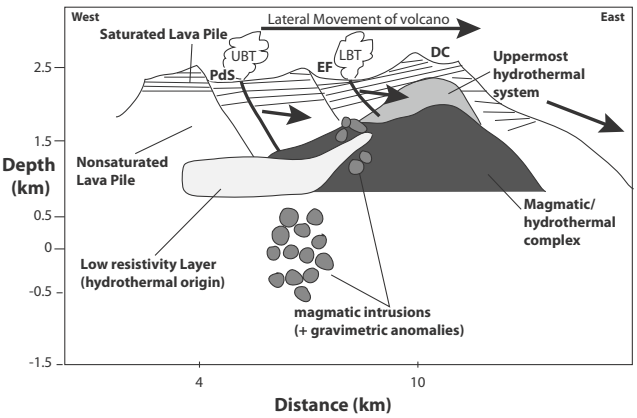

Fig. 7 Cross-sectional model diagram of Piton de la Fournaise summit area, showing the areas from which the Bellecombe eruptions are thought to have originated. Eastward lateral movement of the volcano opened steeply dipping fissures that tapped the hydrothermal and magmatic system under the volcano. The lower Bellecombe eruptions tapped the upper portion of the young hydrothermal system under the Enclos Fouqué caldera as it began to form. The upper Bellecombe eruption included explosions from the more mature hydrothermal system under the Plaine des Sables, where volcanic activity had been centered for millennia prior to the recent migration to the Enclos Fouqué. The subsurface geology is based upon Fontaine et al. (2002). *Heavy arrows* indicate the direction of lateral movement of volcano. Faults thought to have been active in the Bellecombe eruptions are shown by heavier lines and marked LBT (Lower Bellecombe Tephra) and UBT (Upper Bellecombe Tephra) to indicate the associated eruptions. *PdS* Plaine des Sables, *EF* Enclos Fouqué caldera, *CD* Cratère Dolomieu. Depth is shown in kilometers above and below sea level

hydrothermal system, and hot partially degassed lava (perhaps present in the conduit along the new fracture), which were emplaced in the localized breccias and ash of the lower Bellecombe sequence. The abundance of aphyric glassy lava clasts with partially annealed jigsaw cracks is consistent with shallow explosions that broke through near-surface dikes and sills. The presence of hydrothermal quartz indicates that the explosions were in the nonsaturated zone of the hydrothermal system (Fontaine et al. 2002; Bret et al. 2003).

The ash grains in the upper Bellecombe Tephra indicate source depths of 0.5–2.5 km. Dilational movement along a fault again released pressure in the hydrothermal system, which was much older and had altered the rocks more under Plaine des Sables than the new system under Enclos Fouqué (Fontaine et al. 2002) (Fig. 7). The underlying magmatic system, which may have just erupted a significant volume of oceanite, also was involved in the upper Bellecombe eruption, providing abundant juvenile material including aphyric lava, oceanite, and gabbro. This eruption sent clouds of ash <6 km above the vent, and local trade winds carried it to the west and northwest.

Implications for volcanic hazards

Explosive eruptions at other ocean islands have mostly been attributed to phreatomagmatic interactions. The Keanakāko‘i (Swanson et al. 2012a) and Uwēkahuna (Fiske et al. 2009) formations in Hawaii are attributed to phreatic water gaining access to the conduit system, causing explosions; the tephra contains no clay or other evidence for involvement of the hydrothermal system. Similarly, the 2010 Eyjafjallajökull (Gudmundsson et al. 2012) and 2008 Okmok (Larsen et al.

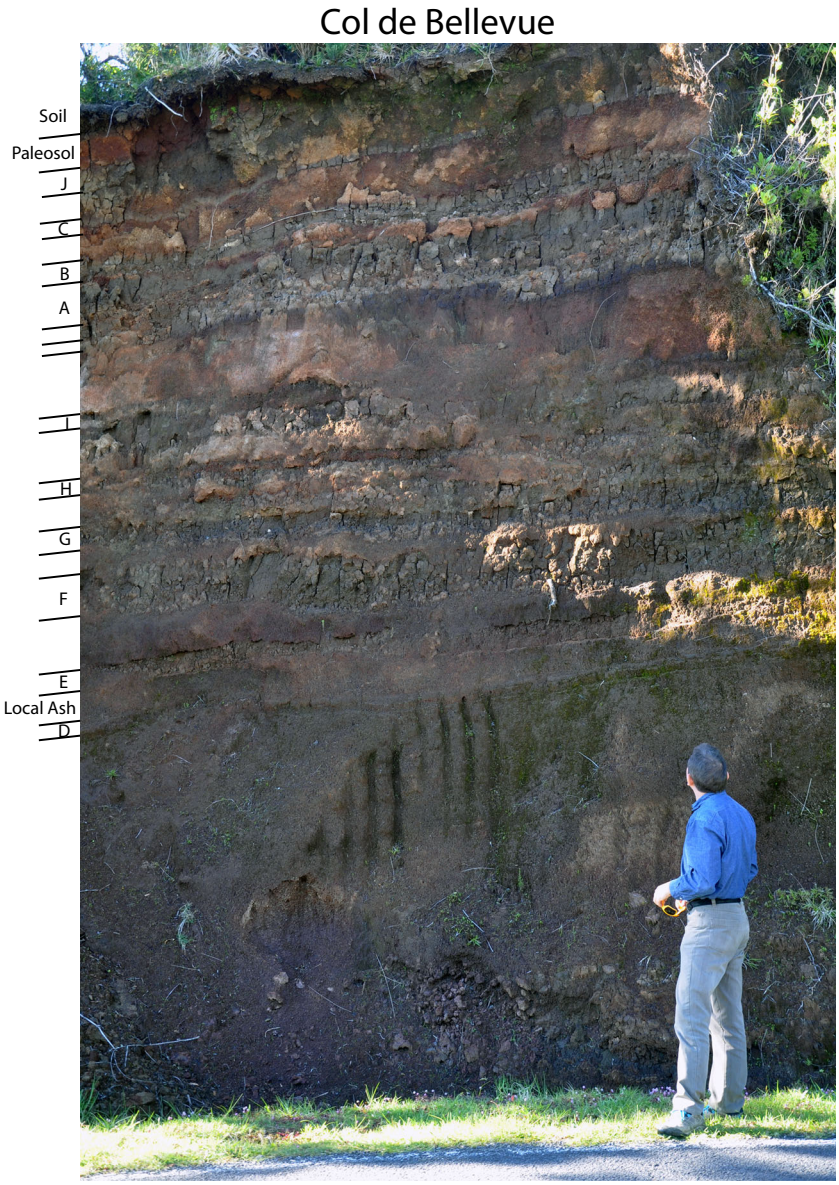

Fig. 8 Photo of thick Bellecombe-like ash deposits near Col de Bellevue. Ash beds are marked. Coarser tephra beds are probably from local scoria cones, but the ash beds were probably erupted from the summit area of Piton de la Fournaise

2009) eruptions produced abundant basaltic ash through the interaction of water (phreatic and ice melt) with magma. However, at Piton de la Fournaise, at least a significant portion of the water for the phreatomagmatism came from the hydrothermal system. We cannot rule out the additional involvement of phreatic water, as it is abundant in the summit area. Small hydrothermal explosions may have occurred frequently since Bellecombe time at Piton de la Fournaise, possibly linked to summit collapses (Michon et al. 2013).

In distal outcrops, 10–11 km downwind from Petite Carrière near Col de Bellevue (Fig. 8), >5 gray ash deposits, each over 30 cm thick, containing laminated fine ash and ash pellet layers are interbedded with local scoria fallouts (Fig. 7). These ash beds have not been dated or correlated to more proximal pyroclastic deposits at PdF. At least some of these ash beds cannot correlate with the Bellecombe Tephra found nearer the vent, but their presence suggests that Bellecombe-like eruptive behavior has been a recurring phenomenon at PdF. In the Piton des Tangues area, a Bellecombe-like unit occurs below the unit dated at 6356 calendar years BP.

The current effusive eruptive style is not the only possibility for the future. Extended eruptions of wet ash could produce lingering hazards in the downwind direction, and lahars could affect inhabited areas at lower elevations, while the associated explosions could make the caldera, a popular tourist destination, hazardous. In 2007, an explosive eruption much smaller than the Bellecombe eruptions severely affected the tourist observation point at the EF rim and sent Pele's hair downwind to Saint Denis on the other side of the island. Fortunately, because the initial caldera collapse occurred at night, no people were present during the explosions. Future explosive eruptions of the size of the Bellecombe events remain both possible and a hazard at Piton de la Fournaise. The potential link between the Bellecombe Tephra and the lateral flank displacements implies a need for thorough monitoring of the flank movement rates. An acceleration in flank displacement may signal a greater likelihood for large seismic events and explosive eruptions.

Acknowledgments This work was supported as part of a national project ("Evaluation de l'alea volcanique à La Réunion" - MEDDTL) to map volcanic hazards of PdF in the last 5000 years. MHO thanks the Institut de Physique du Globe de Paris for a travel grant to work at PdF. Constructive reviews by D. Swanson and M. Gudmundsson and editorial care by G. Giordano greatly improved this manuscript.

References

Anderson K, Wells SG, Graham RC (2002) Pedogenesis of vesicular horizons, Cima Volcanic Field, Mojave Desert, California. Soil Sci Soc Am J 66:878–887

Bachèlery P (1981) Le Piton de la Fournaise (Ile de la Réunion). Etude volcanologique, structurale et pétrologique. Dissertation, University of Clermont-Ferrand.

Bachèlery P, Mairine P (1990) Evolution morphostructurale du Piton de la Fournaise depuis 0,53 Ma. In: Lénat JF (ed) Le volcanisme de l'île de la Réunion. Monographie. Centre de Recherches Volcaniques, Clermont Ferrand, pp 213–242

Bachèlery P, Lénat JF, Di Muro A, Michon L (2015) Piton de la Fournaise and Karthala volcanoes. Springer Active Volcanoes of the World series, Berlin

Boivin P, Bachèlery P (2009) Petrology of 1977 to 1998 eruptions of Piton de la Fournaise, La Réunion Island. J Volcanol Geotherm Res 184:109–125

Bonadonna C, Costa A (2012) Estimating the volume of tephra deposits: a new simple strategy. Geology 40:415–418

Bonadonna C, Costa A (2013) Plume height, volume, and classification of explosive volcanic eruptions based on the Weibull function. Bull Volcanol 75:742. doi:10.1007/s00445-013-0742-1

Brenguier F, Kowalski P, Staudacher T, Ferrazzini V, Lauret F, Boissier P, Catherine P, Lemarchand A, Pequegnat C, Meric O, Pardo C, Peltier A, Tait S, Shapiro NM, Campillo M, Di Muro A (2012) First results from the UnderVolc high resolution seismic and GPS network deployed on Piton de La Fournaise Volcano. Seism Res Lett 83:97–102. doi:10.1785/gssrl.83.1.97

Bret L, Join J-L, Legal X, Coudray J, Fritz B (2003) Argiles et zéolites dans l'altération d'un volcan bouclier en milieu tropical (Le Piton des Neiges, La Réunion). Comptes Rendus Geoscience 335:1031–1038

Di Muro A, Metrich N, Vergani D, Rosi M, Armienti P, Fougeroux T, Deloule E, Arienzo I, Civetta L (2014) The shallow plumbing system of Piton de la Fournaise Volcano (La Reunion Island, Indian Ocean) revealed by the major 2007 caldera-forming eruption. J Petrol 55:1287–1315

Di Muro A, Bachèlery P, Barsotti S, Bielli-Bousquet S, Boissier P, Braukmuller N, Brugier Y, Büttner R, Carey R, Cavalière C, Davoine PA, De Michieli-Vitturi M, Durand J, Frese I, Gurioli L, Mairine P, Marchini G, McPhie J, Métrich N, Michon L, Morandi A, Ort M, Pichavant M, Principe C, Saint-Marc C, Tulet PE, Vergani D, Villeneuve N, Walther G, Wörner G, Zimanowski B (2015) Evaluation de l'aléa volcanique à la Réunion – annéé II. Evaluation of the volcanic hazard at La Réunion - year II. Observatoire Volcanologique du Piton de la Fournaise, report for La Réunion Civil Defense, St Denis, Réunion Island, France, 40 p

Dietze M, Bartel S, Lindner M, Kleber A (2012) Formation mechanisms and control factors of vesicular soil structure. Catena 99:83–96. doi:10.1016/j.catena.2012.06.011

Famin V, Welsch B, Okumura S, Bachèlery P, Nakashima S (2009) Three differentiation stages of a single magma at Piton de la Fournaise (Reunion hotspot). Geochem Geophys Geosyst 10:Q01007. doi:10.1029/2008GC002015

Fiske RS, Rose TR, Swanson DA, Champion DE, McGeehin JP (2009) Kulanaokuaiki Tephra (ca. AD 400–1000): newly recognized evidence for highly explosive eruptions at Kīlauea Volcano, Hawaii. Geol Soc Am Bull 121:712–728

Fontaine FJ, Rabinowicz M, Boulègue J, Jouniaux L (2002) Constraints on hydrothermal processes on basaltic edifices: inferences on the conditions leading to hydrovolcanic eruptions at Piton de la Fournaise, Réunion Island, Indian Ocean. Ear Planet Sci Lett 200:1–14

Fontaine FR, Roult G, Michon L, Barruol G, Di Muro A (2014) The 2007 eruptions and caldera collapse of the Piton de la Fournaise volcano (La Réunion Island) from tilt analysis at a single very broadband seismic station. Geophys Res Lett 41. doi:10.1002/2014GL059691

Gudmundsson MT, Thordarson T, Höskuldsson Á, Larsen G, Björnsson H, Prata FJ, Oddsson B, Magnússon E, Högnadóttir T, Petersen GN, Hayward CL, Stevenson JA, Jónsdóttir I (2012) Ash generation and distribution from the April-May 2010 eruption of Eyjafjallajökull, Iceland. Nature 2:572. doi:10.1038/srep00572

Iverson RM (1995) Can magma-injection and groundwater forces cause massive landslides on Hawaiian volcanoes? J Volcanol Geotherm Res 66:295–308

Join J-L, Folio J-L, Robineau B (2005) Aquifers and groundwater within active shield volcanoes. Evolution of conceptual models in the Piton de la Fournaise volcano. J Volcanol Geotherm Res 147:187–201

Larsen J, Neal C, Webley P, Freymueller J, Haney M, McNutt SR, Schneider D, Prejean S, Schaefer J, Wessels R (2009) Eruption of Alaska volcano breaks historic pattern. Eos Trans AGU 90:173–174

Lénat JF, Fitterman D, Jackson DB, Labazuy P (2000) Geoelectrical structure of the central zone of Piton de la Fournaise Volcano (Reunion). Bull Volcanol 62:75–89

Lénat JF, Bachèlery P, Merle O (2012a) Anatomy of Piton de la Fournaise volcano (La Reunion, Indian Ocean). Bull Volcanol 74:1945–1961

Lénat JF, Bachèlery P, Peltier A (2012b) The interplay between collapse structures, hydrothermal systems, and magma intrusions: the case of the central area of Piton de la Fournaise volcano. Bull Volcanol 74: 407–421. doi:10.1007/s00445-011-0535-3

Martí J, Mitjavila J, Araña V (1994) Stratigraphy, structure and geochronology of the Las Cañadas caldera (Tenerife, Canary Islands). Geol Mag 131:715–727

Mastin LG (1997) Evidence for water influx from a caldera lake during the explosive hydromagmatic eruption of 1790, Kilauea volcano, Hawaii. J Geophys Res 102:20,093–20,109

Mastin LG, Christiansen RL, Thornber C, Lowenstern J, Beeson M (2004) What makes hydromagmatic eruptions violent? Some insights from the Keanakāko'i Ash, Kīlauea Volcano, Hawai'i. J Volcanol Geotherm Res 137:15–31

Mastin LG, Guffanti M, Servranckx R, Webley PW, Barsotti S, Dean K, Denlinger R, Durant A, Ewert JW, Gardner CA, Holliday AC, Neri A, Rose WI, Schneider D, Siebert L, Stunder B, Swanson G, Tupper A, Volentik A, Waythomas CF (2009) A multidisciplinary effort to assign realistic source parameters to model of volcanic ash-cloud transport and dispersion during eruptions. J Volcanol Geotherm Res 186:10–21

McPhie J, Walker GPL, Christiansen RL (1990) Phreatomagmatic and phreatic fall and surge deposits from explosions at Kilauea Volcano, Hawaii, 1790 A.D.: Keanakakoi Ash Member. Bull Volcanol 52: 334–354

Merle O, Mairine P, Michon L, Bachèlery P, Smietana M (2010) Calderas, landslides and paleo-canyons on Piton de la Fournaise volcano (La Réunion Island, Indian Ocean). J Volcanol Geotherm Res 189:131–142. doi:10.1016/j.jvolgeores.2009.11.001

Michon L, Saint-Ange F (2008) The morphology of Piton de la Fournaise basaltic shield volcano (La Réunion island): characterization and implication in the volcano evolution. J Geophys Res 113:B03203. doi:10.1029/2005JB004118

Michon L, Staudacher T, Ferrazzini V, Bachèlery P, Martí J (2007) April 2007 collapse of Piton de la Fournaise: A new example of caldera formation. Geophys Res Lett 34:L21301. doi:10.1029/2007GL031248

Michon L, Di Muro A, Villeneuve N, Saint-Marc C, Fadda P, Manta F (2013) Explosive activity of the summit cone of Piton de la Fournaise volcano (La Réunion island): A historical and geological review. J Volcanol Geotherm Res 263:117–133

Michon L, Ferrazzini V, Di Muro A, Villeneuve N, Famin V (2015) Rift zones and magma plumbing system of Piton de la Fournaise volcano: how do they differ from Hawaii and Etna. J Volcanol Geotherm Res 303:112–129. doi:10.1016/j.jvolgeores.2015.07.031

Mohamed-Abchir A (1996) Les Cendres de Bellecombe: un évènement majeur dans le passé récent du Piton de la Fournaise, Ile de la Réunion. Dissertation, Université de Paris VII.

Mohamed-Abchir A, Semet SM, Boudon G, Ildefonse P, Bachèlery P, Clocchiati R (1998) Huge hydrothermal explosive activity on Piton de la Fournaise, Réunion Island: The Bellecombe ash member, 2700 BC. In: Casal R, Fytikas M, Sigvaldasson G, Vougioukalakis G (eds) Volcanic Risk—The European Laboratory Volcanoes. Eur Comm, Brussels, pp 447–455

Morandi A, Principe C, Di Muro A, Leroi G, Michon L, Bachèlery P (2016) Pre-historic explosive activity at Piton de La Fournaise volcano. In: Bachèlery P, Lénat JF, Di Muro A, Michon L (eds) Active Volcanoes of the Southwest Indian Ocean: Piton de la Fournaise and Karthala. Active Volcanoes of the World. Springer-Verlag, Berlin and Heidelberg, pp 107–138

Rose WI, Durant AJ (2011) Fate of volcanic ash: Aggregation and fallout. Geology 39:895–896. doi:10.1130/focus092011.1

Roult G, Peltier A, Taisne B, Staudacher T, Ferrazzini V, Di Muro A, the OVPF team (2012) A new comprehensive classification of the Piton de la Fournaise activity spanning the 1985–2010 period. Search and analysis of short-term precursors from a broad-band seismological station. J Volcanol Geotherm Res 241–242:78–104

Schumacher R, Schmincke H-U (1995) Models for the origin of accretionary lapilli. Bull Volcanol 56:626–639

Sparks RSJ, Bursik MI, Carey SN, Gilbert JE, Glaze L, Sigurdsson H, Woods AW (1997) Volcanic Plumes. John Wiley and Sons, Chichester, 574 p

Staudacher T, Allègre CJ (1993) Ages of the second caldera of Piton de la Fournaise volcano (Réunion) determined by cosmic ray produced ^{3}He and ^{21}Ne. Earth Planet Sci Lett 119:395–404

Swanson DA (2008) Hawaiian oral tradition describes 400 years of volcanic activity at Kīlauea. J Volcanol Geotherm Res 176:427–431

Swanson DA, Rose TR, Fiske RS, McGeehin JP (2012a) Keanakāko i Tephra produced by 300 years of explosive eruptions following collapse of Kīlauea's caldera in about 1500 CE. J Volcanol Geotherm Res 215–216:8–25

Swanson DA, Zolkos SP, Haravitch B (2012b) Ballistic blocks around Kīlauea Caldera: Their vent locations and number of eruptions in the late 18th century. J Volcanol Geotherm Res 231–232:1–11

Swanson DA, Rose TR, Mucek AE, Garcia MO, Fiske RS, Mastin LG (2014) Cycles of explosive and effusive eruptions at Kīlauea Volcano, Hawai'i. Geology 42:631–634. doi:10.1130/G35701.1

Swanson DA, Weaver SJ, Houghton BF (2015) Reconstructing the deadly eruptive events of 1790 at Kīlauea Volcano, Hawai'i. Geol Soc Am Bull 127:503–515. doi:10.1130/B31116.1

Tulet P, Villeneuve N (2011) Large scale modeling of the transport, chemical transformation and mass budget of the sulfur emitted during the April 2007 eruption of Piton de la Fournaise. Atmos Chem Phys 11:4533–4546. doi:10.5194/acp-11-4533-2011

Upton BGJ, Semet MP, Joron J-L (2000) Cumulate clasts in the Bellecombe Ash Member, Piton de la Fournaise, Réunion Island, and their bearing on cumulative processes in the petrogenesis of the Réunion lavas. J Volcanol Geotherm Res 104:297–318